Supporting Information for

Dual-protection of graphene-sulfur composite by a compact graphene skin and an atomic layer deposited oxide coating for lithium-sulfur battery

Mingpeng Yu,[a] Aiji Wang,[b] Fuyang Tian,[c] Hongquan Song,[c] Yinshu Wang, [b] Chun Li,[a] Jong-Dal Hong,[d] and Gaoquan Shi*[a]

[a]Department of Chemistry, Tsinghua University, Beijing 100084, People's Republic of China. Fax: 86 62771149; Tel: 86 6277 3743; E-mail: gshi@tsinghua.edu.cn
[b]Department of Physics, Beijing Normal University, Beijing 100875, People's Republic of China
[c]Institute for Applied Physics, University of Science and Technology Beijing, Beijing 100083, People's Republic of China
[d]Department of Chemistry, Incheon National University, 406-772 Incheon, South Korea

1. ALD of ZnO and MgO onto G−S composites

ZnO or MgO film was deposited onto G–S aerogel by using an ALD system of SUNALE R200 (Picosun). In the case of preparing ZnO/G–S, a piece of G–S aerogel was placed in the ALD chamber where zinc diethyl ($Zn(C_2H_5)_2$, 99.9999%, Jiangsu Nata Opto-electronic Material Co. Ltd) reacted with H_2O to form ZnO for 40 ALD cycles. The operational pressure of the ALD system was maintained at about 1800-2000 Pa and the temperature was kept at 120°C throughout the deposition. For preparing MgO/G–S, bis(ethylcyclopentadienyl) magnesium ($Mg(CpEt)_2$, 99.9999%, Jiangsu Nata Opto-electronic Material Co. Ltd) was used as the precursor and the other conditions were the same to those described above.

2. Morphological studies of the electrodes after long-term tests

The Li–S cells after charging/discharging at 0.2 C for 100 cycles were disassembled in a glove box and the cathodes were thoroughly washed with dimethyl carbonate and dried before SEM characterization.

3. Summary of the active sulfur loading in various Li-S battery systems

Table S1

Cathode	Sulfur loading	Reference
Sulfur–TiO_2 yolk–shell nanocomposite	0.4-0.6 mg cm^{-2}	*Nat. Commun.*, 2013, **4**, 1331.
CNF-encapsulated Sulfur cathode	1 mg cm^{-2}	*Nano Lett.*, 2011, **11**, 4462.
Amphiphilic surface-modified CNF-Sulfur composite	1 mg cm^{-2}	*Nano Lett.*, 2013, **13**, 1265.
CTAB-modified Sulur−GO nanocomposite	0.8 mg cm^{-2}	*Nano lett.*, 2013, **13**, 5891.
PVP-encapsulated hollow Sulfur composite	1 mg cm^{-2}	*PNAS*, 2013, **110**, 7148.
RGO@MWCNTs-W/Sulfur composite	0.8-0.9 mg cm^{-2}	*J. Power Sources*, 2014, **253**, 55.
G-KBC/Sulfur composite	1.5 mg cm^{-2}	*ACS Appl. Mater. Interfaces*, 2014, **6**, 10917.
RGO/Sulfur	1 mg cm^{-2}	*Adv. Energy Mater.*, 2014, 1400482
pPAN–Sulfur@GNS	0.752 mg cm^{-2}	*ChemSusChem*, 2014, **7**, 563.
Sulfur/CNT	1-1.5 mg cm^{-2}	*Energy Environ. Sci.*, 2012, **5**, 8901.
Li_2S–polypyrrole	1 mg cm^{-2}	*Energy Environ. Sci.*, 2014,**7**, 672.
Sulfur-impregnated N-doped carbon	1 mg cm^{-2}	*ChemElectroChem*, 2014, **1**, 1040.

4. Theoretical calculations

All calculations were carried out by the use of DMol3 program package.[S1] The exchange and correlation potential was calculated by using the generalized gradient approximation (GGA) of Perdew and Wang (PW91).[S2] The valence electron functions were expanded into a set of numerical atomic orbitals by a double-numerical basis with polarization functions (DNP). The convergence criterions of optimal geometry are 1×10^{-5} Hartree for total energy, 2×10^{-3} Hartree for force and 5×10^{-4} nm for displacement convergence. All of the computations were

performed with spin-polarization.

Considering the accuracy and efficiency of calculation, we modelled the ZnO(0001) surface by a periodic four-bilayer slab with a p (3 × 3) unit cell (Fig. S7) and the MgO(001) surface by a periodic five-layer slab with a p (√2× √2) unit cell (Fig. S8). One molecule was adsorbed on one side of these slabs. The vacuum region thickness between the repeat slabs was set to be 1.2 nm to avoid the interactions between different slabs. In the process of the simulation, the Li-S• molecule and the two layers on the top of the slab were allowed to relax freely, while the other four layers at bottom were fixed.

Theoretical calculations indicate that the binding energies of the sulfur containing species with ZnO and MgO are 5.404 and 1.220 eV, respectively.

5. Supplementary figures

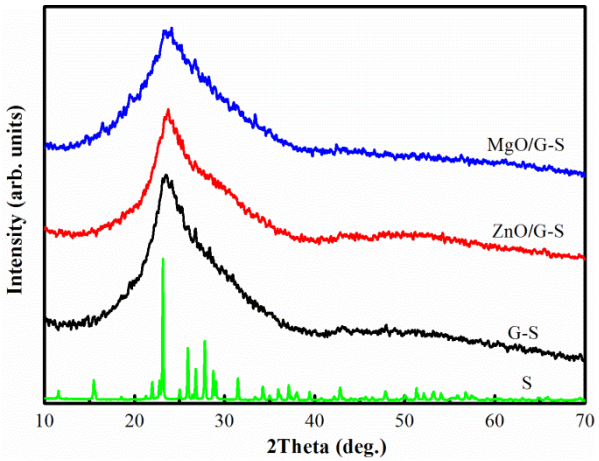

Fig. S1 XRD patterns of S powder, and G–S, ZnO/G−S and MgO/G−S composites.

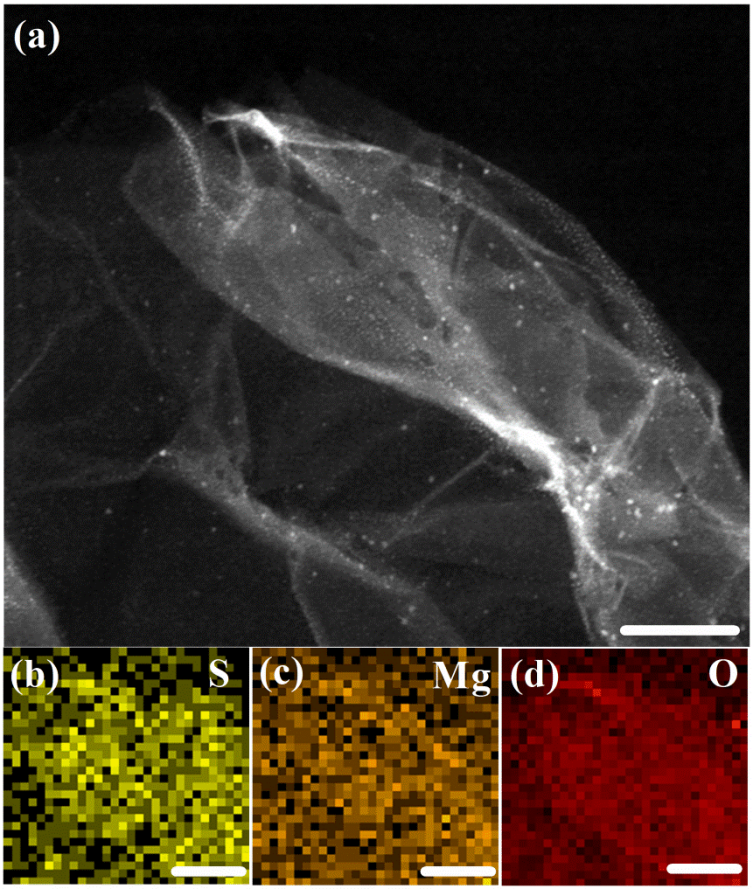

Fig. S2 (a) STEM image of MgO/G−S composite and the corresponding elemental mapping images of (b) sulfur, (c) magnesium and (d) oxygen. Scale bars, 100 nm.

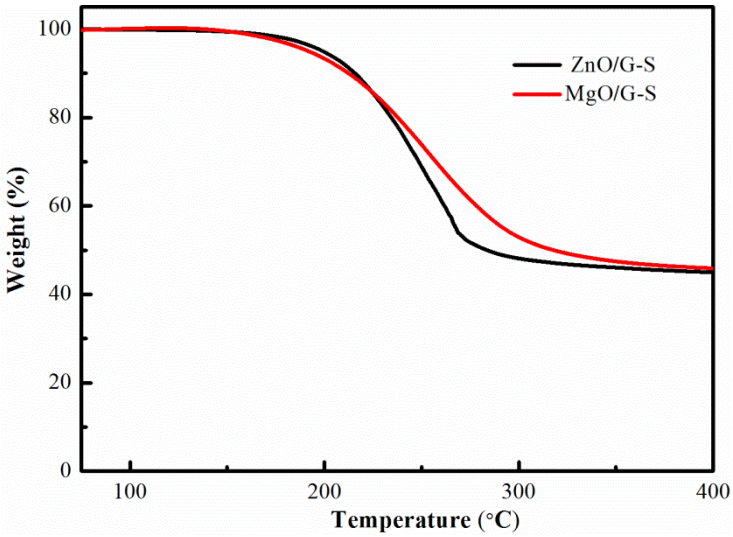

Fig. S3 Thermal gravity analysis (TGA) curves of ZnO/G−S and MgO/G−S composites.

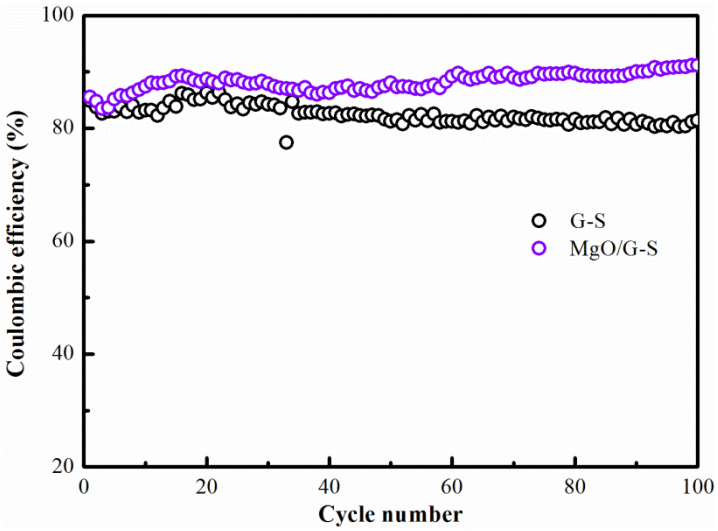

Fig. S4 Coulombic efficiencies of the G–S and MgO/G–S composites during the process of charging/discharging at 0.2 C for 100 cycles.

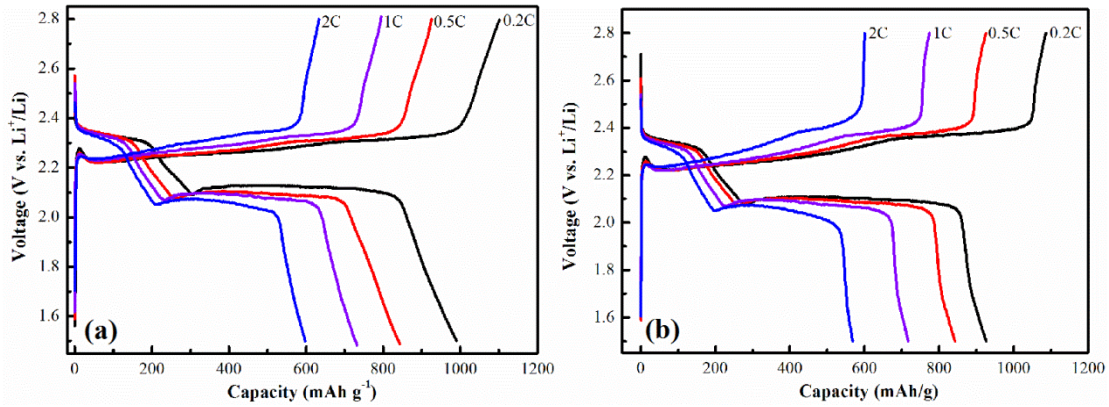

Fig. S5 The initial charge–discharge profiles of (a) ZnO/G–S and (b) MgO/G–S composites. The plateaus of ZnO/G–S electrode are flat and stable with a relatively lower polarization (the voltage difference between the charging and discharging curves at given rate and capacity) compared with that of MgO/G–S electrode.

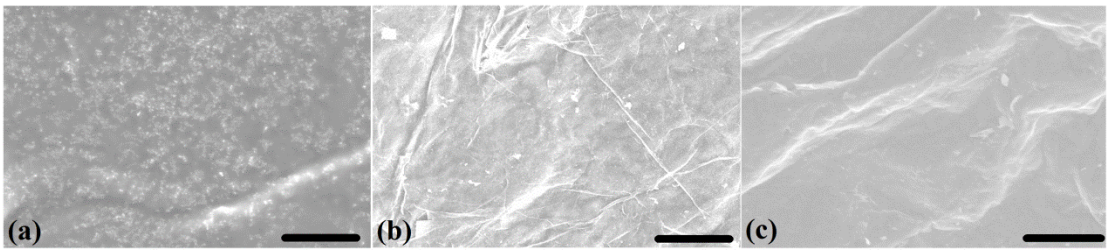

Fig. S6 SEM images of the skin layers for (a) G–S, (b) MgO/G–S and (c) ZnO/G–S composite electrodes after 100 cycles at 0.2 C. Scale bars, 10 μm.

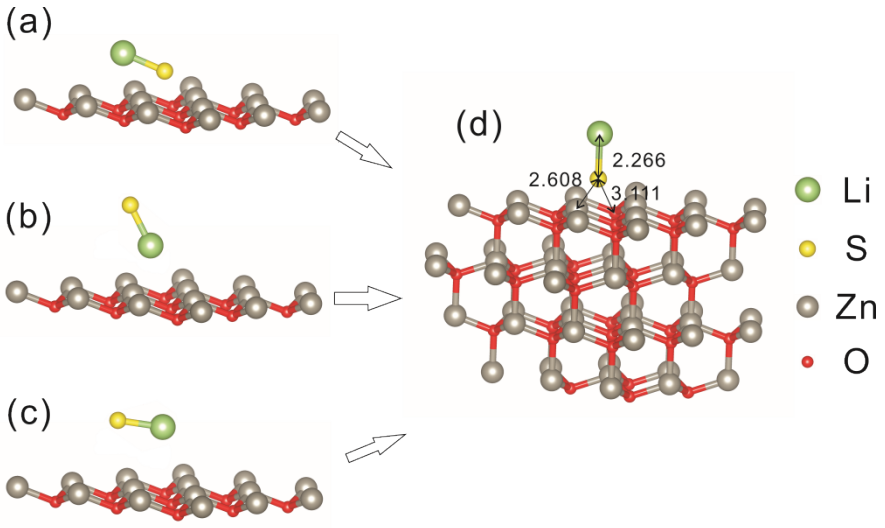

Fig. S7 The configuration of LiS on ZnO(0001) surface: (a), (b), and (c) are the initial geometries, and (d) is the optimal geometry.

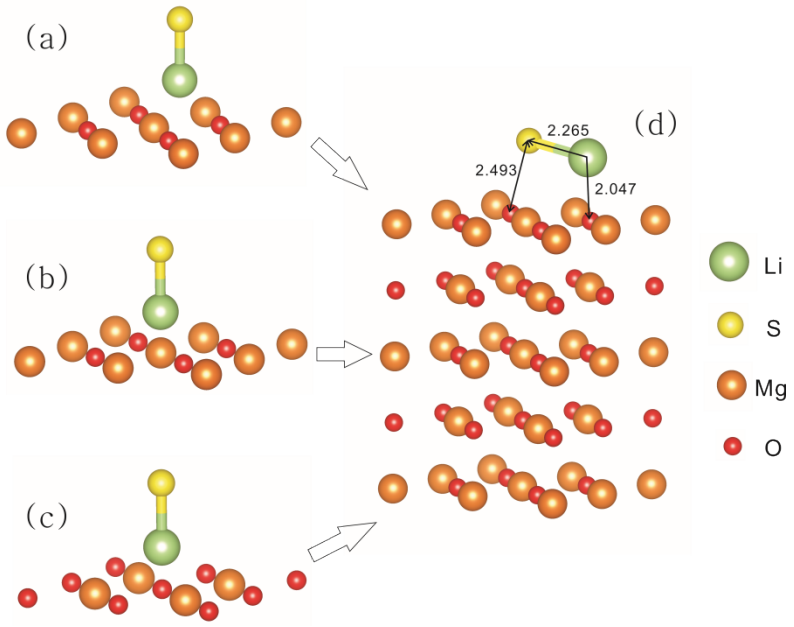

Fig. S8 The configuration of LiS on MgO(001) surface: (a), (b), and (c) are the initial geometries, and (d) is the optimal geometry.

S1 B. Delley, *J. Chem. Phys*., 2000, **113**, 7756.

S2 J. P. Perdew, J. A. Chevary, S. H. Vosko, K. A. Jackson, M. R. Pederson, D. J. Singh, and C. Fiolhais, *Phys. Rev. B,* 1992, **46**, 6671.